ROYAL SOCIETY
OF CHEMISTRY

PAPER

Check for updates

The development of a novel bio-based corrosion inhibitor: using biomass-derived 5-hydroxymethylfurfural (5-HMF) as a starting material†

Kexin Liu,‡[a] Ping Li,‡[a] Xia Li,[b] Wei Zhang,[c] Jiawei Zou,[a] Yuan Liu,[a] Pengyu Li,[a] Haitao Cui,[a] Yu Yang*[a] and Wenying Ai [ID] *[a]

An environmentally friendly corrosion inhibitor was prepared from the bio-based platform 5-hydroxymethylfurfural. This corrosion inhibitor was confirmed to be an efficient mixed-type corrosion inhibitor through a weight loss experiment and electrochemical experiment. Both thermodynamic and kinetic parameters were calculated and discussed, indicating that the adsorption of this bio-based inhibitor on a steel surface is a chemisorption process. Moreover, quantum chemical calculations were performed and further confirmed the formation of an effective productive film of this bio-based inhibitor on the metal surface. It is worth noting that the synthesis route of this bio-based corrosion inhibitor is green and environmentally friendly, and does not involve toxic chemical reagents.

Introduction

Biomass is considered to be a unique renewable carbon resource, which can be generated directly from crop wastes, plant raw materials, and industrial residues.[1] Utilization of biomass sources for the production of value-added bio-based fuels, chemicals and polymer precursors has attracted much attention due to its carbon-neutral properties, and the abundant reserves.[2] 5-Hydroxymethylfurfural (5-HMF) is a promising bio-based platform, which is synthesized from biomass, and considered as a bridge between biomass resources and petrochemical resources.[3] 5-HMF has been applied to the formation of various chemical products,[4] such as fuels, perfumes, pharmaceuticals, agrochemicals, and polymers. In addition, 5-HMF is an excellent precursor for many valuable monomers (*e.g.* FDCA, *etc.*). Although there have been a lot of reports on the value-added conversion of 5-HMF, the utilization of 5-HMF in the field of metal corrosion protection has not been fully researched.

Mild steel is widely used in various fields of industry, such as chemical processing, petroleum production, and marine applications, due to its excellent mechanical properties.[5] Metal corrosion can result in serious economic losses and safety hazards to the production, because of the effect of acid picking and other processes.[6] Many strategies have been employed in these processes to protect metals against corrosion and control the corrosion rate.[7] Among these strategies, the corrosion inhibitor is considered to be a convenient, green and environment-friendly method.[6]

Corrosion inhibitors can be divided into inorganic inhibitors and organic inhibitors.[8] The inorganic inhibitors are usually displayed high toxicity and harmful to the environment, such as mercury salt, nitrite,[9] and phosphate.[10] Compared with inorganic corrosion inhibitors, the organic inhibitors are usually eco-friendly to the natural environment. Most organic inhibitors contain heteroatoms (nitrogen, oxygen, sulfur and phosphorus) with lone pair of electrons and/or aromatic rings with π electrons.[11–13] And these inhibitors are adsorbed on the metallic surface through interaction to block the active corrosion sites. Nevertheless, the complex synthetic methods, by-products and high cost severely limited the application of organic corrosion inhibitors. Therefore, the development of an environmental and ecological conscious corrosion inhibitor has become the research direction in this field recently.[14]

Herein, we developed a novel bio-based corrosion inhibitor (furylalkonium chlorid, compound **1b**) originating from 5-HMF *via* two steps of organic transformations (Schemes 1 and 2). The structure skeleton of this bio-based inhibitor contains a quaternary ammonium salt substituent, aldehyde, and furyl group,

[a]*School of Material and Chemical Engineering, Zhongyuan University of Technology, Zhengzhou, Henan Province 450007, People's Republic of China. E-mail: 6786@zut.edu.cn*

[b]*Department of Pharmacy, Logistics University of People's Armed Police Forces, Tianjin Key Laboratory for Prevention and Control of Occupational and Environmental Hazard, Tianjin, 300309, China*

[c]*Zhejiang Sugar Energy Technology Co., Ltd., Ningbo New Material Innovation Center, A1-6, High-tech Zone, East District, Ningbo, Zhejiang Province 315100, China*
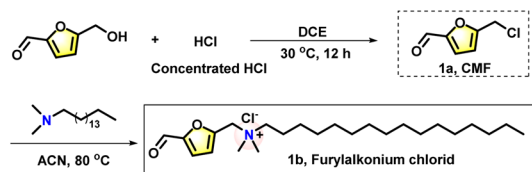
† Electronic supplementary information (ESI) available. See DOI: https://doi.org/10.1039/d3ra08240g

‡ These authors contributed equally to this work.
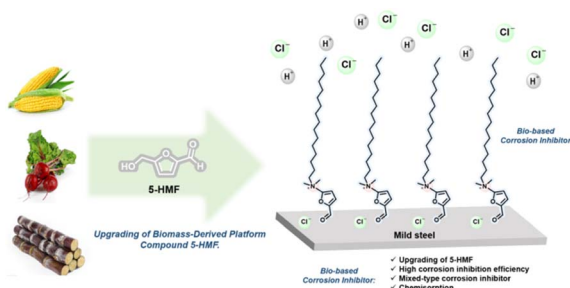
Scheme 1 Schematic illustration of this work.

Scheme 2 The synthetic method and structural formula of furylalkonium chlorid.

which can adsorb on the metal surface through (1) the electrostatic attraction between the N^+ terminal in quaternary ammonium salt and the negative charged metal originating from the adsorption of chloride anions; (2) unshared electron pairs of the O atom in furyl ring and aldehyde group with the vacant 3d-orbital of the Fe atom which leads coordination adsorption of the bio-based corrosion inhibitor, ultimately forming a dense hydrophobic film on the metal surface; (3) the interaction between the π-electrons of furyl and the vacant d-orbital of iron atom in the metal. Besides, the long carbon chains of inhibitor molecules can effectively hinder the corrosion of carbon steel by corrosive ions due to the hydrophobicity of the long carbon chains. Corrosion experiments and polarization measurements on mild steel in 0.5 M HCl solution indicate that the corrosion inhibitor is an efficient mixed corrosion inhibitor. The polarization resistance increases with increasing concentration of corrosion inhibitor furylalkonium chlorid.

Experimental

The synthetic procedure of 5-CMF

The important intermediate 5-CMF was prepared from 5-HMF (1 g, 8 mmol) through a substitution step. To the solution of 5-HMF in 1,2-dichloroethane (35 mL), was added con. HCl (20 mL) dropwise at 0 °C. And then the solution was stirred at room temperature for 12 h. The reaction was quenched by water (100 mL). The organic phase was dried by Na_2SO_4, and then concentrated in vacuum to give the crude product **1a**, which can be used directly in the next step.

The synthetic procedure of target product furylalkonium chlorid

To the solution of **1a** (1 g, 772 μl, 7 mmol) in acetonitrile, was added *N,N*-dimethylhexadecan-1-amine at room temperature,

and then the reaction was stirred at 80 °C for 1 h. After that, the solution was concentrated directly to generate the crude product, which was subjected to column chromatography to give the target bio-based corrosion inhibitor furylalkonium chlorid (the yield of these two steps is 85%).

Mild steel samples with dimensions 50 mm × 25 mm × 2 mm were polished with different grades of emery papers (grade 400-1000-2000). Then the samples were washed with double-distilled water and anhydrous ethanol. After that, the specimens were dried and weighed before being immersed in corrosive solutions with different concentrations of corrosion inhibitor (0 ppm, 1 ppm, 3 ppm, 5 ppm, and 10 ppm) at 303 K, 313 K and 323 K for 4 hours, respectively. Afterwards, the mild steel samples were washed with distilled water and ethanol. Finally, the samples were weighed again and dried at room temperature. We repeated each experiment three times and then afforded the average value of mass loss before and after immersing the mild steel in the corrosive media.

Electrochemical experiment

All the electrochemical experiments described in this paper were recorded using CHI660E electrochemical instrumentation. Potentiodynamic polarization measurement and electrochemical impedance spectroscopy (EIS) were performed using a conventional three-electrode system assembly in which a calomel electrode was used as the reference electrode, a mild steel electrode covered with epoxy resin (steel with an exposed area of 0.5 cm²) was used as the working electrode, and a platinum plate was used as the counter electrode. We first immersed the working electrodes in the test solution for 3 hours to produce a stable open-circuit potential. Electrochemical impedance spectroscopy (EIS) was then performed at the open-circuit potential (E_{OCP}) using a 10 mv signal across the frequency range of 100 Hz to 0.01 Hz. Next, potentiodynamic polarization measurements were performed in the potential range of ±250 mV *vs.* E_{OCP} at the scan rate of 1 mV s⁻¹.

The cyclic voltammetry experiments were performed using a three electrode cell (volume 15 mL) with a Pt plate counter electrode, glassy carbon working electrode (diameter 5 mm), and Ag/AgNO₃ (0.1 M AgNO₃ in CH₃CN solution) reference electrode. In all cases, the CV experiments were conducted in DMSO containing 0.1 M Bu₄NClO₄ as supporting electrolyte. Sample concentration was 10 mM, scan speed 0.1 V s⁻¹. Before every measurement cycle, the measurement solution was purged with nitrogen gas for 5 min to remove O_2. For each sample, two CV cycles were collected, and to keep consistency, only the first CV cycle was used for further analysis.

Quantum chemical calculation

Quantum chemical calculations were carried out by using Gaussian 09 and the optimized molecular structure of the bio-based corrosion inhibitor was generated based on density functional theory by using a B3LYP-D3 with 6-311 ++ G(d, p). In addition, we calculated quantum chemical parameters, such as, E_{HOMO}, E_{LUMO}, and μ, which represent the highest occupied

molecular orbital energy, the lowest unoccupied molecular orbital energy, and the dipole moment, respectively.

Results and discussion

Weight loss experiment

Weight loss experiments were conducted to determine the corrosion inhibition capacity of the bio-based corrosion inhibitor furylalkonium chlorid. The results for mild steel samples in the 0.5 M HCl solution with and without inhibitor at different temperatures were displayed in Fig. 1, respectively. The corrosion rate (V) and the corrosion inhibition efficiency ($\eta\%$) of the mild steel specimens were calculated as follow:

$$V = \frac{8.76 \times 10^4 \times \Delta W}{s \times t \times \rho} \tag{1}$$

$$\eta\% = \frac{V_0 - V}{V_0} \times 100\% \tag{2}$$

where ΔW denotes the weight loss of the samples before and after soaking; s means the total surface area; ρ represents the density of the sample (7.85 g cm^{-3}); t is the immersing time; and V_0 and V are the corrosion rates of the specimen in the corrosive solution without and with inhibitor, respectively.

As depicted in the Fig. 1, the corrosion inhibition efficiency ($\eta\%$) of the bio-based corrosion inhibitor decreased with rising temperature, which could be ascribed to the desorption of initially adsorbed bio-based inhibitor molecules. And the corrosion rate of the samples in the inhibited solutions was slower than that observed in the blank solution, which suggested that the furylalkonium chlorid showed high corrosion inhibition capacity. Besides, the weight loss experiments of furylalkonium chlorid were conducted in higher concentration of corrosive media (1 M HCl) at 303 K for 4 h to determine the corrosion inhibition capacity again. Evident from these values, only a very low concentration of compound furylalkonium chlorid is required to give high efficiency (Table S1†).
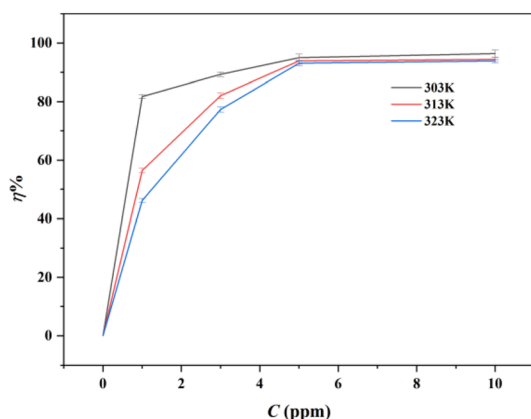

Fig. 1 The corrosion inhibition efficiency for the mild steel in 0.5 M HCl containing different concentrations of inhibitor furylalkonium chlorid with at 303 K, 313 K and 323 K, respectively.

Potentiodynamic polarization measurement

The corrosion inhibition ability of the bio-based corrosion inhibitor furylalkonium chlorid was further investigated by potentiodynamic polarization measurement. Fig. 2a showed the potentiodynamic polarization curves of mild steel in 0.5 M HCl solutions containing different concentrations of inhibitor furylalkonium chlorid at 303 K. Parameters generated from the potentiodynamic polarization curves, such as, corrosion potential (E_{corr}), corrosion current density (I_{corr}), cathodic Tafel slope (β_c), anodic Tafel slope (β_a), and corrosion inhibition efficiency ($\eta_{Tafel}\%$), are listed in Table 1. The corrosion inhibition efficiency ($\eta_{Tafel}\%$) is calculated by the following expression:

$$\eta_{Tafel}\% = \frac{I_{corr}^0 - I_{corr}}{I_{corr}^0} \times 100\% \tag{3}$$

where I_{corr}^0 and I_{corr} represent corrosion current densities without and with corrosion inhibitor, respectively.

As depicted in Fig. 2a, the addition of bio-based corrosion inhibitor furylalkonium chlorid caused the decrease of the corrosion current density (I_{corr}), which indicated that the inhibitor furylalkonium chlorid reduced the corrosion rate of the steel samples efficiently. This result was attributed to the formation of a complete and stable adsorption film on the surface of steel samples, and the film hinders the reaction between the corrosive ions in the acid solution and the surface of mild steel. In addition, a small positive shift (28.9 mV, less than 85 mV) was observed in the measurement of the corrosion potential for inhibitor furylalkonium chlorid. When the shift value of corrosion potential is greater than 85 mV, the corrosion inhibitor could be classified as an anode or cathode type inhibitor; and when the value of the maximum shift in corrosion potential is less than 85 mV,[15] the inhibitor could be considered as a mixed-type corrosion inhibitor.[15]

EIS measurement

Fig. 2b–d give the Nyquist and Bode plots of the tested mild steel in 0.5 M HCl solution in the absence and presence of corrosion inhibitor furylalkonium chlorid at 303 K, respectively. As displayed in Fig. 2b, the Nyquist plot shows a capacitive loop at high frequencies (HFs), and the diameter of the HF capacitive loop increases with the addition of inhibitor concentration, which indicates that the high inhibition ability of the bio-based corrosion inhibitor furylalkonium chlorid. The capacitive loop is typically related to the charge transfer resistance and the double layer capacitance.[16] The capacitive loops showed as depressed semicircles, which may be attributed to the frequency dispersion because of the nonhomogeneity and roughness of the working electrode surface.[17] According to Fig. 2c, the impedance modulus increased with the inhibitor concentration increasing.

As presented in Fig. 3, the electrical equivalent circuit was employed to simulate the impedance data of furylalkonium chlorid. In the circuit, R_s is the solution resistance, R_{ct} is the charge transfer resistance, and Q_{dl} represents the constant phase element and can be described as follows:

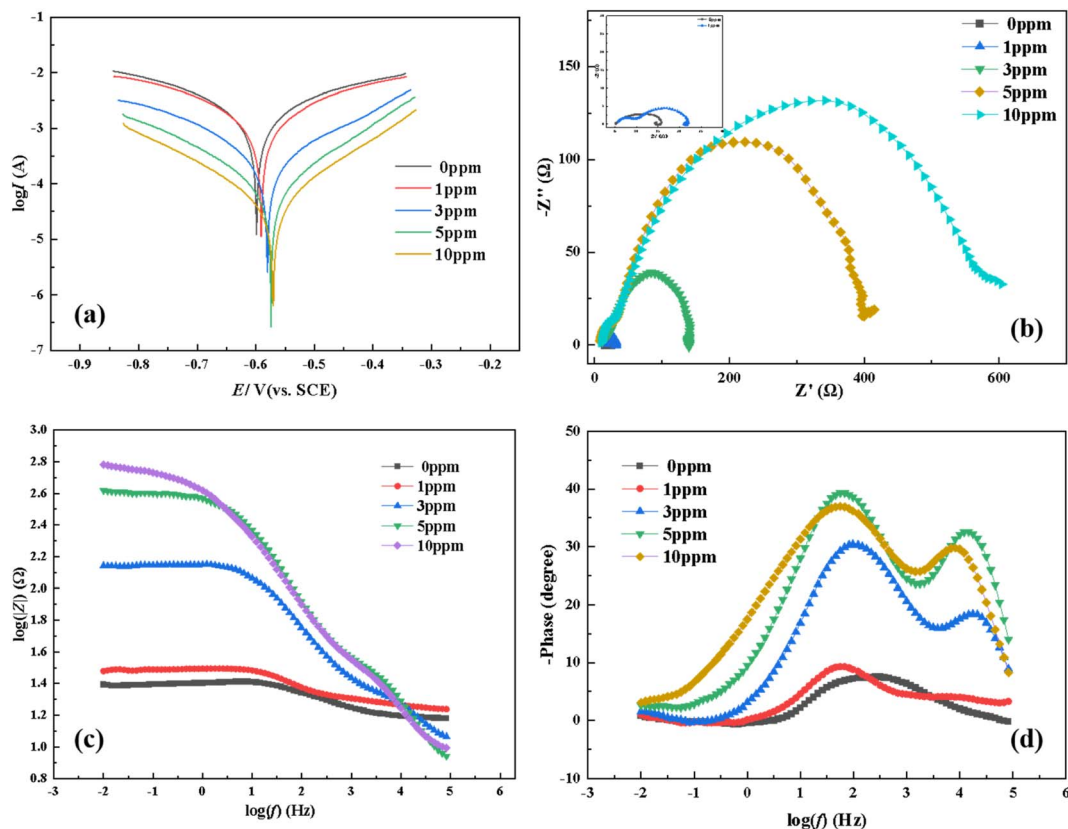$$Z_{Q_{dl}} = \frac{1}{Y_0(j\omega)^n} \tag{4}$$

Fig. 2 Potentiodynamic polarization curves (a), Nyquist plots (b), and Bode plots (c and d) for mild steel in 0.5 M HCl solution with different concentrations of furylalkonium chlorid at 303 K.

Table 1 Electrochemical parameters for steel specimens in the 0.5 M HCl solution containing different concentrations of furylalkonium chlorid

C (ppm)	E_{corr} (V)	I_{corr} (mA cm^{-2})	$-b_c$ (mV dec^{-1})	b_a (mV dec^{-1})	h_{Tafel} (%)
0	−0.5990	1.590	187.8640	203.3347	—
1	−0.5905	0.7513	136.7802	93.6768	52.7
3	−0.5803	0.2569	153.8462	176.5225	83.8
5	−0.5907	0.0806	150.1276	136.3884	94.9
10	−0.5701	0.0451	146.8644	137.5327	99.7

where Y_0 denotes the Q_{dl} constant, j denotes the imaginary number, ω denotes the angular frequency, and n denotes the phase shift that can be considered as a degree of surface inhomogeneity.

In addition, the suppression efficiency $(\eta_{Rct}\%)$ obtained from the EIS measurements were calculated as follow:

$$\eta_{R_{ct}}\% = \frac{R_{ct} - R_{ct}^0}{R_{ct}} \times 100\% \qquad (5)$$

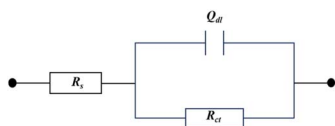Herein, R_{ct} and R_{ct}^0 are the charge transfer resistance with and without corrosion inhibitor furylalkonium chlorid respectively.

Table 2 represents the impedance parameters generated from electrical equivalent circuits. The results showed that the addition of inhibitor furylalkonium chlorid increased the values of R_{ct} compared with the blank solution. And the corrosion inhibition efficiency $(\eta_{R_{ct}}\%)$ of furylalkonium chlorid at 10 ppm reaches 99.2%, which suggested that increasing the inhibitor concentration could promote the formation of productive films on metal sample surfaces, thus improving inhibition efficiency.

Surface analysis and water contact angle (WCA)

Fig. 4a and b gives the surface morphologies of mild steel samples after corrosion in 0.5 M HCl solution with and without 10 ppm inhibitor furylalkonium chlorid for 4 h at 303 K. The

Fig. 3 Simulated equivalent circuit.

Table 2 The EIS parameters for mild steel in 0.5 M HCl solution with different concentration of furylalkonium chlorid at 303 K

| C (ppm) | R_s (Ω cm^2) | Q_{dl} | | R_{ct} (Ω cm^2) | η_{Rct} (%) |
		Y_0 (μF cm^{-2})	n		
0	7.679	13.23×10^{-4}	0.6940	4.962	—
1	17.91	0.1508×10^{-4}	0.6203	13.53	63.3
3	12.79	4.308×10^{-4}	0.5478	138.2	96.4
5	6.602	4.038×10^{-4}	0.4827	459.3	98.9
10	7.375	5.353×10^{-4}	0.4697	658.9	99.2
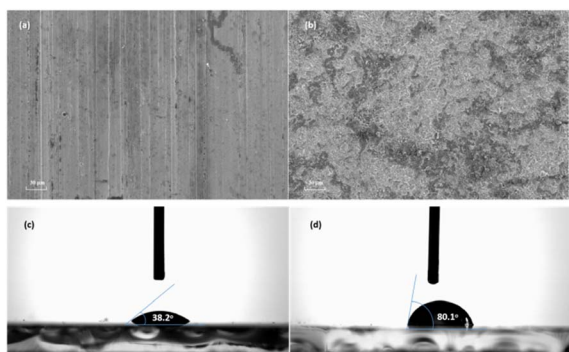
Fig. 4 SEM images of the sample surface after corrosion in 0.5 M HCl solution with 10 ppm furylalkonium chlorid (a), and without inhibitor for 4 h at 303 K (b); WCA images of glass surface (immersed in water) without inhibitor (c), and with 0.75 M inhibitor (d).

morphology in Fig. 4b shows a highly damaged surface, characteristic of the corrosion of metal sample in 0.5 M HCl solution. In the presence of inhibitor furylalkonium chlorid, a smoother surface is observed, which indicated that the surface was protected by compound furylalkonium chlorid. In addition, contact angle measurements were conducted to determine the degree of wettability of compound furylalkonium chlorid. According to Fig. 4c and d, the glass substrate that was exposed to water without inhibitor was observed a WCA of 38.2°. And the WCA was observed to rise by 80.1° when the glass surface contained 0.75 M inhibitor furylalkonium chlorid, suggesting that the glass surface became extremely hydrophobic. This was caused by the formation of the absorption film of furylalkonium chlorid.

Adsorption isotherms

The adsorption isotherm can provide significant information about the inhibition mechanism between the corrosion inhibitor molecules and the metal surface. In order to model the adsorption of corrosion inhibitor furylalkonium chlorid on the mild steel surface, the Langmuir isotherm equation was used to fit the experimental results of the surface coverage measured by loss weight experiments. The following equation was used to calculate the Langmuir isotherm:

$$\frac{C}{\theta} = \frac{1}{K} + C \tag{6}$$

Herein, C represents the concentration of the corrosion inhibitor, θ represents the surface coverage of the corrosion inhibitor molecules and the value of θ is equal to the weight loss corrosion inhibition efficiency (η%), K represents the adsorption isotherm constant.

In addition, the corresponding standard free energy (ΔG^0_{ads}), enthalpies (ΔH^0_{ads}), and entropies (ΔS^0_{ads}) for adsorption of furylalkonium chlorid on metal surfaces can be generated by the following expressions, respectively:

$$\Delta G^0_{ads} = -RT \ln(55.5K) \tag{7}$$

$$\frac{\Delta G_{ads}{}^0}{T} = \frac{\Delta H_{ads}{}^0}{T} + k \tag{8}$$

$$\Delta S_{ads}{}^0 = \frac{\Delta H_{ads}{}^0 - \Delta G_{ads}{}^0}{T} \tag{9}$$

Herein, T stands for the absolute temperature, the value 55.5 is the molar concentration of water in the solution, and R stands for the molar gas constant. The Langmuir isothermogram and the corresponding thermodynamic parameters are shown in Fig. 5 and Table 3

The plots of C with C/θ show a good linear relationship at different temperatures as shown in Fig. 5a, indicating that the adsorption of inhibitor furylalkonium chlorid on mild steel follows the Langmuir isothermal model. In addition, the adsorption parameters, including K, ΔG^0_{ads}, ΔH^0_{ads} and ΔS^0_{ads} are shown in Table 3. The values of K decrease with increasing the temperature, which indicates that adsorption of inhibitor furylalkonium chlorid on the metal surface is unfavorable at higher temperature, and could explain the decrease in the
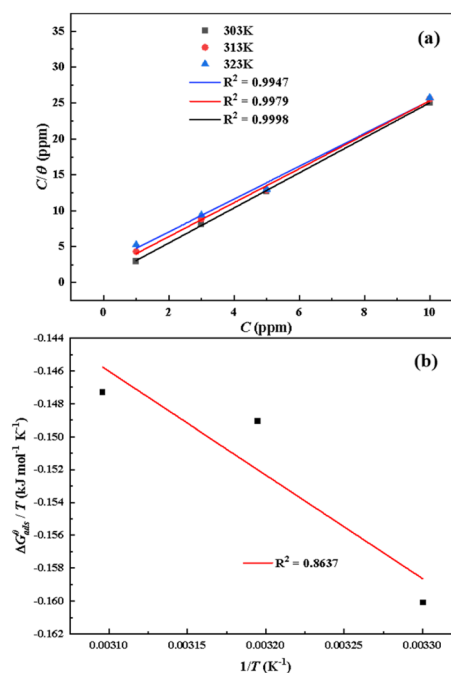
Fig. 5 (a) Langmuir adsorption isotherm plots of the inhibitor furylalkonium chlorid on metal steel surface; (b) curves of $\Delta G^0_{ads}/T$ versus $1/T$.

Table 3 Thermodynamic parameters for the adsorption of furylalkonium chlorid on metal steel

T (K)	K (mol^{-1} L)	ΔG_{ads}^0 (kJ mol^{-1})	ΔH_{ads}^0 (kJ mol^{-1})	ΔS_{ads}^0 (J mol^{-1} K^{-1})
303	4.1506×10^6	-48.5064	-63.0584	-48.0262
313	1.1008×10^6	-46.6534		-52.4119
323	0.8911×10^6	-47.5764		-47.9318

corrosion inhibition efficiency with the increase of temperature. It is noted the values of ΔG_{ads}^0 are less than -40 kJ mol^{-1}, which indicated that the adsorption of the corrosion inhibitor furylalkonium chlorid on the metal surface is chemisorption.[18] The plot of $\Delta G_{ads}^0/T$ versus $1/T$ yields a straight line has been depicted in Fig. 5b. According to eqn (8), the value of ΔH_{ads}^0 is equal to the slope of the straight line ($\Delta G_{ads}^0/T$ vs. $1/T$) and it is less than zero, which suggested the adsorption of furylalkonium chlorid on the metal surface is an exothermic process. The values of ΔS_{ads}^0 for inhibitor furylalkonium chlorid are negative, which can be explained by a decrease of adsorbed molecule's translation freedom.[11]

Activation parameters

In order to further investigate the inhibition mechanism of corrosion inhibitor furylalkonium chlorid, the effect of temperature on the metal corrosion rate in 0.5 M HCl solutions with and without inhibitor furylalkonium chlorid was investigated by utilizing the Arrhenius and transition state equations, respectively:

$$\ln V = -\frac{E_a}{RT} + \ln A \qquad (10)$$

$$V = \left(\frac{RT}{Nh}\right)\exp\left(\frac{\Delta S^{\neq}}{R}\right)\exp\left(\frac{-\Delta H^{\neq}}{RT}\right) \qquad (11)$$

where E_a is the apparent activation energy, R is the universal gas constant, A is the pre-exponential factor, h stands for the Planck's constant, N is Avogadro's number, V is the corrosion rate, $\Delta S^{\neq}$ is the apparent entropy of activation, and $\Delta H^{\neq}$ is the apparent enthalpy of activation.

Fig. 6a and b give Arrhenius and transition state plots for steel samples immersed in 0.5 M HCl solution with and without inhibitor furylalkonium chlorid, respectively. The obtained plots are straight lines, therefore, the kinetic parameters, such as, E_a, $\Delta H^{\neq}$ and $\Delta S^{\neq}$ are calculated based on the slopes and intercepts of these straight lines, and these results are listed in Table 4. Obviously, the values of E_a and $\Delta H^{\neq}$ follow the same trend in the tested solutions and the values of them in the inhibited solutions are greater than the values obtained from blank solution. This result can be explained by the known thermodynamic equation $\Delta H^{\neq} = E_a - RT$. And the values of E_a in the inhibited solutions are higher than in blank solution, which suggested that the dissolution of metal samples is slow in inhibited solution because of the adsorption of inhibitor molecules.[19] In addition, the values of $\Delta S^{\neq}$ in the inhibited solutions are greater than blank solution, which indicated that an increase in disorder occurs during the transition from the reactant to activated complex in the corrosion process.[20]
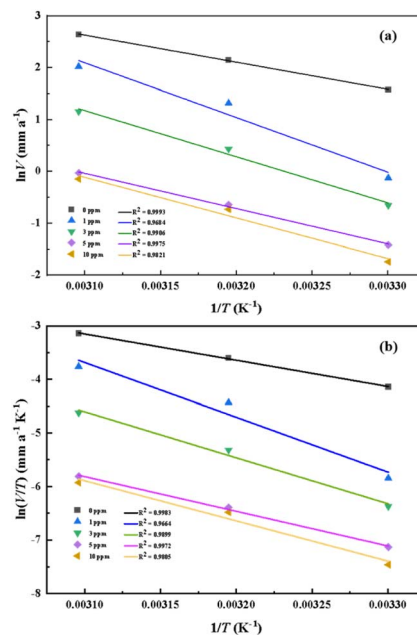
Fig. 6 Arrhenius plots (a) and transition state plots (b) for metal steel in 0.5 M HCl solution with different concentrations of furylalkonium chlorid.

Quantum chemical calculations

Quantum chemical calculations were performed to further understand the inhibition mechanism of bio-based corrosion inhibitor furylalkonium chlorid. To evaluate the effect of solvation, we calculate the HOMO and LUMO energies of furylalkonium chlorid theoretically in DMSO (PCM model). The optimized geometric structure and the electron density distribution of HOMO and LUMO for furylalkonium chlorid are depicted in Fig. 7. The quantum chemical parameters, such as, E_{HOMO}, E_{LUMO}, and the HOMO–LUMO gap (ΔE), are given in Table 5. Based on the frontier molecular orbital theory, the foundation of the transition state is attributed to a HOMO–

Table 4 Activation parameters for mild steel in 0.5 M HCl solution with different concentrations of furylalkonium chlorid

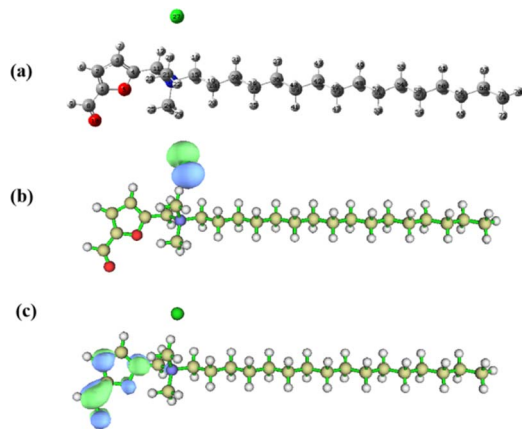| C (ppm)	E_a (kJ mol^{-1})	$\Delta H^{\neq}$ (kJ mol^{-1})	$\Delta S^{\neq}$ (kJ mol^{-1} K^{-1})
0	43.4002	40.80013	-174.75397
1	87.6674	85.06732	-41.96085
3	73.9497	71.34965	-92.14341
5	56.5101	53.91	-156.27137
10	65.0541	62.45407	-130.42564

Fig. 7 Optimized geometric structure (a) and the distributions of HOMO (b) and LUMO (c) for inhibitor furylalkonium chlorid.

Fig. 8 Mulliken and NPA charge distribution on bio-based inhibitor furylalkonium chlorid.

Table 5 The HOMO and LUMO energies of furylalkonium chlorid obtained from CV experiments and DFT quantum chemical calculations

Method	E_{HOMO} (eV)	E_{LUMO} (eV)	ΔE (eV)
DFT	−6.82	−2.53	4.29
CV	−5.32	−3.33	1.99

LUMO interaction of reactants.[21,22] As depicted in Fig. 7b and c, the electron density distribution of HOMO for furylalkonium chlorid is mainly located on the chloride anion, and that of LUMO for furylalkonium chlorid is mainly located on the aldehyde group. Besides, we use cyclic voltammetry experiments to get the real E_{LUMO} and E_{HOMO} to compare with the theoretical value (Table 5). As the processes involved being irreversible, the anodic and cathodic peak potential of compound furylalkonium chlorid were measured separately. Calculation of HOMO and LUMO energy levels is carried out according to the oxidation potential and reduction potential presented in Fig. S10† by using the following equations:[23,24]

$$E_{HOMO} = -E^{ox} + E_{1/2}(Fc/Fc^+) - IP(Fc) \qquad (12)$$

$$E_{LUMO} = -E^{red} + E_{1/2}(Fc/Fc^+) - IP(Fc) \qquad (13)$$

where E^{ox} is the oxidation onset, E^{red} is the reduction onset and $E_{1/2}(Fc/Fc^+)$ is the half-wave potential of ferrocene (0.0555 V). The energy value of the Fc/Fc$^+$ redox system is assumed to be IP(Fc) = 4.8 eV below the vacuum level.

As presented in Table 5, there is some deviation in the energy values of the HOMO and LUMO of inhibitor furylalkonium chlorid obtained from CV and quantum chemical calculations. This result may be caused by the cationic feature of inhibitor furylalkonium chlorid.[25] Generally, E_{HOMO} is always associated with the electron-donating ability of the molecule, and a high E_{HOMO} value indicates a strong electron-donating ability.[26] E_{LUMO} is related to the electron-accepting ability of the molecule, and a low the value of E_{LUMO} signifies a high electron-
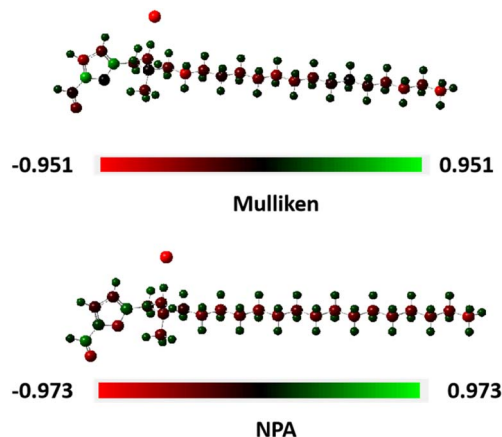
accepting ability. And it is studied previously that the low value of HOMO–LUMO gap ΔE is responsible for the high inhibition efficiency.[26] Therefore, the most probable adsorption mode of furylalkonium chlorid, is that, chloride ions are first adsorbed on the metal surface, then, the quaternary ammonium salt cation part of furylalkonium chlorid adsorbs on the steel surface via the electrostatic interaction. The lone pair electrons of O atoms in furyl ring and aldehyde group might be transferred to the vacant 3d-orbital of Fe atom to form a coordinate bond. Moreover, the π-electrons of furyl group could also interact with the vacant 3d-orbital of Fe atom in the mild steel.

This adsorption process can be further confirmed by the Mulliken and NPA charge distribution of inhibitor furylalkonium chlorid.[27] To evaluate the effect of solvation, the charge distribution of furylalkonium chlorid was also calculated theoretically in DMSO (PCM model). In Fig. 8, red part stands for the negative regions in molecule furylalkonium chlorid, and green part represents the positive regions. Obviously, the 5O and 10O atoms of furyl ring and aldehyde groups in furylalkonium chlorid are negatively charged, which further proved that the negatively charged 5O and 10O atoms serve as the electron donors to give their lone pair electrons to the vacant 3d-orbital of Fe atom forming a coordinate bond with the metal surface. In addition, the NPA charge density of 27Cl atom was over −0.3 eV, too. Hence, chloride ions of furylalkonium chlorid are first adsorbed on the steel surface, and then the absorption film could be formed by the electrostatic interaction between chloride ions and quaternary ammonium salt cation of furylalkonium chlorid.

Conclusions

Herein, we report the design and synthesis of an environment-friendly and novel corrosion inhibitor from the bio-based platform compound 5-hydroxymethylfurfural in this manuscript. This may become a new research direction for the value-added utilization of 5-HMF in the field of energy and green chemistry. The weight loss experiments, electrochemical experiments indicated this corrosion inhibitor an efficient

mixed-type corrosion inhibitor.The adsorption of this bio-based inhibitor on steel surface was confirmed to be a chemisorption progress by calculating the thermodynamic and kinetic parameters. In addition, the quantum chemical calculations were used to investigate the probable inhibition mechanism of the bio-based corrosion inhibitor. Notably, the synthetic method of this bio-based corrosion inhibitor is environment-friendly, and doesn't involve the use of toxic chemical reagents.

Data availability

Data will be made available on request.

Conflicts of interest

There are no conflicts to declare.

Acknowledgements

Notes and references

1 Q. Hou, X. Qi, M. Zhen, H. Qian, Y. Nie, C. Bai, S. Zhang, X. Bai and M. Ju, *Green Chem.*, 2021, **23**, 119–231.

2 N. Luo, T. Montini, J. Zhang, P. Fornasiero, E. Fonda, T. Hou, W. Nie, J. Lu, J. Liu, M. Heggen, L. Lin, C. Ma, M. Wang, F. Fan, S. Jin and F. Wang, *Nat. Energy*, 2019, **4**, 575–584.

3 B. Saha and M. M. Abu-Omar, *Green Chem.*, 2014, **16**, 24–38.

4 P. Maneechakr and S. Karnjanakom, *React. Chem. Eng.*, 2020, **5**, 2058–2063.

5 P.-E. Aba-perea and E. Becker, *J. Mater. Process. Technol.*, 2020, **283**, 116717.

6 D. A. Winkler, *Metals*, 2017, **7**, 553.

7 M. Rbaa, F. Benhiba, A. S. Abousalem, M. Galai, Z. Rouifi, H. Oudda, B. Lakhrissi, I. Warad and A. Zarrouk, *J. Mol. Struct.*, 2020, **1213**, 128155.

8 H. Li, Y. Zhang, C. Li, Z. Zhou, X. Nie, Y. Chen, H. Cao, B. Liu, N. Zhang, Z. Said, S. Debnath, M. Jamil, H. M. Ali and S. Sharma, *Korean J. Chem. Eng.*, 2022, **39**, 1107–1134.

9 G. Gece, *Corros. Sci.*, 2011, **53**, 3873–3898.

10 S. Mandal, J. K. Singh, D.-E. Lee and T. Park, *Materials*, 2020, **13**, 3642.

11 M. V. Fiori-Bimbi, P. E. Alvarez, H. Vaca and C. A. Gervasi, *Corros. Sci.*, 2015, **92**, 192–199.

12 F. Zhang, Y. Tang, Z. Cao, W. Jing, Z. Wu and Y. Chen, *Corros. Sci.*, 2012, **61**, 1–9.

13 Z. Zhang, N. Tian, L. Zhang and L. Wu, *Corros. Sci.*, 2015, **98**, 438–449.

14 J. Kaur, N. Daksh and A. Saxena, *Arabian J. Sci. Eng.*, 2022, **47**, 57–74.

15 F. Cui, Y. Ni, J. Jiang, L. Ni and Z. Wang, *Chem. Eng. Commun.*, 2021, **208**, 1580–1593.

16 A. Kosari, M. H. Moayed, A. Davoodi, R. Parvizi, M. Momeni, H. Eshghi and H. Moradi, *Corros. Sci.*, 2014, **78**, 138–150.

17 K. Khaled, *Mater. Chem. Phys.*, 2011, **125**, 427–433.

18 J. Lazrak, E. Ech-chihbi, R. Salim, T. Saffaj, Z. Rais and M. Taleb, *Colloids Surf., A*, 2023, **664**, 131148.

19 J. Jennane, M. E. Touhami, S. Zehra, Y. Baymou, S.-H. Kim, I.-M. Chung and H. Lgaz, *Mater. Chem. Phys.*, 2019, **227**, 200–210.

20 T. Lu and F. Chen, *J. Comput. Chem.*, 2012, **33**, 580–592.

21 M. Fedel, M. Poelman, M. Olivier and F. Deflorian, *Surf. Interface Anal.*, 2019, **51**, 541–551.

22 T. Lu and F. Chen, *J. Comput. Chem.*, 2012, **33**, 580–592.

23 A. B. Khelifa, K. Ezzayani, M. Guergueb, F. Loiseau, E. Saint-Aman and H. Nasri, *J. Mol. Struct.*, 2021, **1227**, 129508.

24 M. Soltani, R. Minakar, H. R. Memarian and H. Sabzyan, *J. Phys. Chem. A*, 2019, **123**, 2820–2830.

25 A. V. Kulinich, N. A. Derevyanko, A. A. Ishchenko, N. B. Gusyak, I. M. Kobasa, P. P. Romańczyk and S. S. Kurek, *Dyes Pigm.*, 2019, **161**, 24–33.

26 X. Zheng, S. Zhang, W. Li, M. Gong and L. Yin, *Corros. Sci.*, 2015, **95**, 168–179.

27 G. Xia, X. Jiang, L. Zhou, Y. Liao, M. Duan, H. Wang, Q. Pu and J. Zhou, *J. Ind. Eng. Chem.*, 2015, **27**, 133–148.